Observation of octupole excitations in ^{141}Cs and ^{143}Cs nuclei

W. Urban and T. Rząca-Urban
Institute of Experimental Physics, Warsaw University, ul. Hoża 69, 00-681 Warsaw, Poland

J. L. Durell, W. R. Phillips, A. G. Smith, and B. J. Varley
Schuster Laboratory, Department of Physics and Astronomy, University of Manchester, Manchester M13 9PL, United Kingdom

N. Schulz
Institut de Recherches Subatomiques UMR7500, CNRS-IN2P3 et Université Louis Pasteur, 67037 Strasbourg, France

I. Ahmad
Argonne National Laboratory, Argonne, Illinois 60439, USA
(Received 3 March 2003; published 30 January 2004)

Excited states in ^{141}Cs and ^{143}Cs, populated in spontaneous fission of ^{248}Cm, were studied by means of prompt-γ spectroscopy, using the EUROGAM2 multidetector array. This work reports the first observation of octupole excitations in the ^{141}Cs and ^{143}Cs nuclei. The new data for ^{141,143}Cs do not support theoretical predictions of octupole deformation in the neutron-rich Cs isotopes and indicates octupole correlations weaker than observed in the corresponding Ba isotones.

DOI: 10.1103/PhysRevC.69.017305 PACS number(s): 23.20.Lv, 21.60.Cs, 25.85.Ca, 27.60.+j

Studies of neutron-rich lanthanides have revealed a region of octupole instability around $N=88$ [1,2]. A key question concerns the extent of this region. Calculations of Ref. [3] suggested that the neutron-rich Cs isotopes have an octupole deformation in their ground states. In our previous studies of these nuclei [4], done using EUROGAM1, we have identified yrast excitations in ^{141}Cs, ^{143}Cs, and ^{145}Cs, interpreted as either decoupled (^{141,143}Cs) or strongly coupled (^{145}Cs) configurations, due to valence protons in the $\pi g_{7/2}$ and $\pi d_{5/2}$ orbitals. No octupole excitations were found and no conclusions could be drawn about the strength of octupole correlations in these nuclei. Other studies [5,6] also did not report any octupole effects there. Our next measurement of prompt γ rays from fission of ^{248}Cm, performed using the EUROGAM2 array, provided much higher statistics (for details of the experiment see, e.g., Ref. [7]). Using the new data we uncovered many new γ transitions in ^{141}Cs and ^{143}Cs, extended their excitation schemes and identified levels corresponding to octupole excitations, as discussed in details below. Partial results of these investigations were reported in Ref. [8].

Figure 1 shows some of the analyzed coincidence spectra, double gated on the known and the newly identified transitions in ^{141}Cs. Based on such spectra, 14 new γ lines, deexciting new nonyrast levels in ^{141}Cs, were found in the present work.

Figure 2 shows the new level scheme of ^{141}Cs, as obtained in this work. To the scheme reported in Ref. [4] we add levels at 1549.7 1632.0, 1661.0, 1941.2, 2000.6, 2086.5, 2465.2, 2648.1, 2675.0, and 2994.4 keV, based on the observed coincidence relations. We could not confirm the 1577.2 keV level reported in Ref. [6] because our data suggest that the 726.7 keV line reported in Ref. [6] feeds the 1488.8 keV level, rather than the 850.7 keV level.

Spin and parity $7/2^+$ for the ground state and $5/2^+$ for the 105.7 keV level were taken from the literature [4,5]. Spins and parities of other levels in ^{141}Cs were deduced from γ-γ angular correlations [9,10], obtained in this work and shown in Table I as well as from decay properties of the levels and from previous works [4,5]. Since no half-life longer than 10 ns was seen, the quadrupole transitions observed in ^{141}Cs and ^{143}Cs are $E2$.

The total conversion coefficient for the 105.7 keV transition, found from the intensity balance, is $\alpha_T=1.5(2)$. This value can be compared to the theoretical values of 0.2, 0.9, and 1.7 for the $E1$, $M1$, and $E2$ multipolarities, respectively, confirming the $M1+E2$ character of the 105.7 keV transition.

Figure 3 shows the new level scheme of ^{143}Cs, as obtained in this work. To the scheme reported in Refs. [4,6] we add 17 new, nonyrast levels, based on the observed coincidence relations, some of which are shown in Fig. 4. Figure 4(a) illustrates a new band based on the 1182.3 keV level. Figure 4(b) indicates the assignment of the 404.9 keV and 628.8 keV transition to ^{143}Cs. Similarly, the spectra shown in Figs. 4(c) and 4(d) support the introduction of other new transitions in ^{143}Cs.

We adopt spin $3/2^+$ for the ground state from the literature [4]. Spins and parities of other levels in ^{143}Cs, shown in Fig. 3 were deduced in this work from γ-γ angular correlations and directional-polarization correlations of the observed γ transitions, shown in Table II, and from decay properties of the levels in ^{143}Cs.

An important result of this work is an $E1$ multipolarity assignment to the 399.6 keV, 523.5 keV, and 628.8 keV transitions, based on the angular correlation and linear polarization. This allows the negative-parity assignment to the bands based on the 816.6 keV and 872.6 keV levels.

With a negative-parity assignment to the new bands in ^{143}Cs, based on the 816.6 keV and 872.6 keV levels, a parity-doublet-like structure is found in this nucleus. It is expected that in nuclei with octupole deformation, one

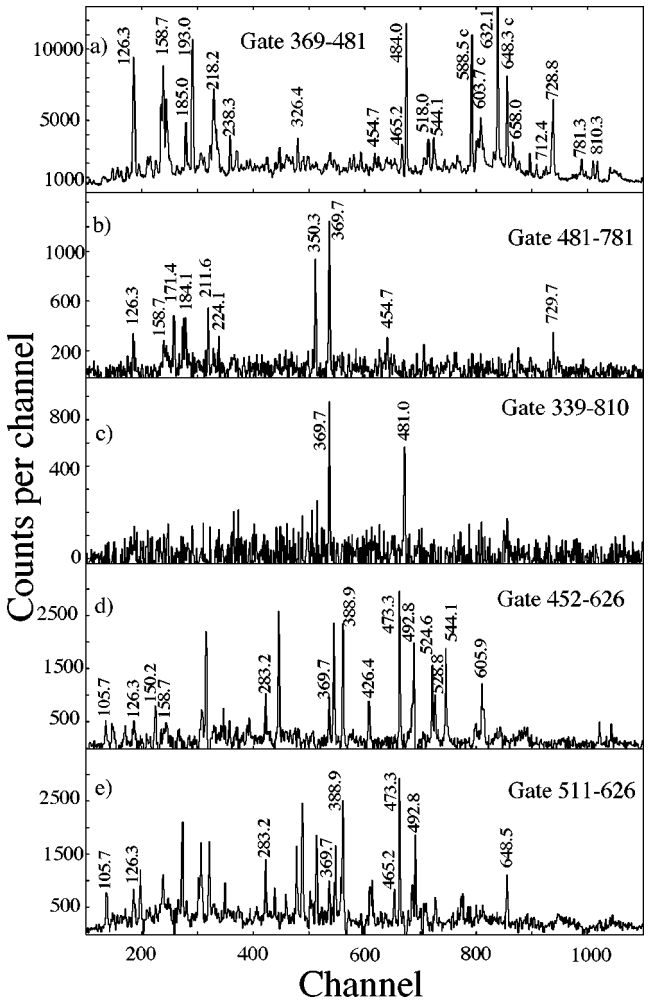

FIG. 1. Coincidence spectra gated on lines corresponding to γ transitions in the ^{141}Cs nucleus, as obtained in this work. Unlabeled lines do not belong to ^{141}Cs and are due to gate contaminations. Label "*c*" denotes a complex line.

TABLE I. Angular correlation values for transitions in the ^{141}Cs nucleus. "Sum" denotes the summed correlation with several yrast, quadrupole transitions.

$E_{\gamma 1}-E_{\gamma 2}$ (keV−keV)	A_2/A_0	A_4/A_0	Multipolarity of γ_1 transition
105.2−283.2	−0.10(3)	0.07(4)	$\Delta I=2$
283.2−473.3	0.12(2)	−0.08(6)	$\Delta I=2$
388.9−473.3	−0.07(2)	0.06(4)	$\Delta I\leqslant 1$
452.6−626.5	−0.06(2)	0.04(4)	$\Delta I\leqslant 1$
481.0−369.7	0.09(2)	−0.04(2)	$\Delta I=2$
492.8−369.7	−0.11(3)	0.08(5)	$\Delta I\leqslant 1$
603.7−sum	−0.07(2)	0.01(3)	$\Delta I\leqslant 1$
626.5−sum	0.08(2)	−0.04(4)	$\Delta I=2$
632.1−sum	0.10(2)	−0.07(4)	$\Delta I=2$
648.3−sum	0.11(3)	−0.03(3)	$\Delta I=2$
810.3−sum	−0.14(3)	0.06(3)	$\Delta I\leqslant 1$

should observe electric dipole moments D_0 significantly larger than in nuclei without octupole deformation. Neutron-rich barium isotopes ^{142}Ba and ^{144}Ba are good example [11]. It is interesting to compare D_0 moments in Cs nuclei with values in their Ba isotones.

In Table III we show $B(E1)/B(E2)$ branching ratios for ^{143}Cs and tentative $B(E1)/B(E2)$ branching ratios for ^{141}Cs. In ^{141}Cs the parity-doublet-like structure is hardly seen. We took dipole/quadrupole branchings for the 2086.5 keV and 2465.2 keV levels, assuming that these levels have negative parity. From that, tentative values of $B(E1)/B(E2)$ branching ratios in ^{141}Cs were obtained. The $B(E1)/B(E2)$ branching ratios can be used to estimate electric dipole moments in both nuclei using the rotational formula $D_0 = \sqrt{5B(E1)/16B(E2)}\times Q_0$. The electric quadrupole moments

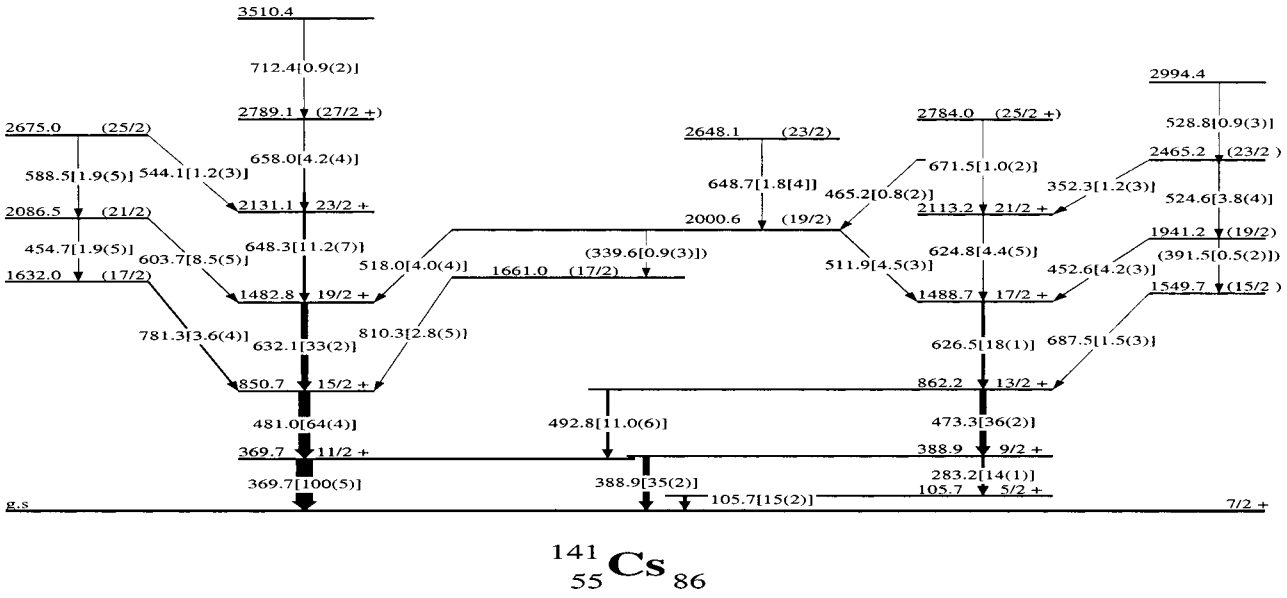

FIG. 2. Partial level scheme of ^{141}Cs as obtained in the present work. In square brackets relative γ intensities are given. Transitions in round brackets are placed tentatively.

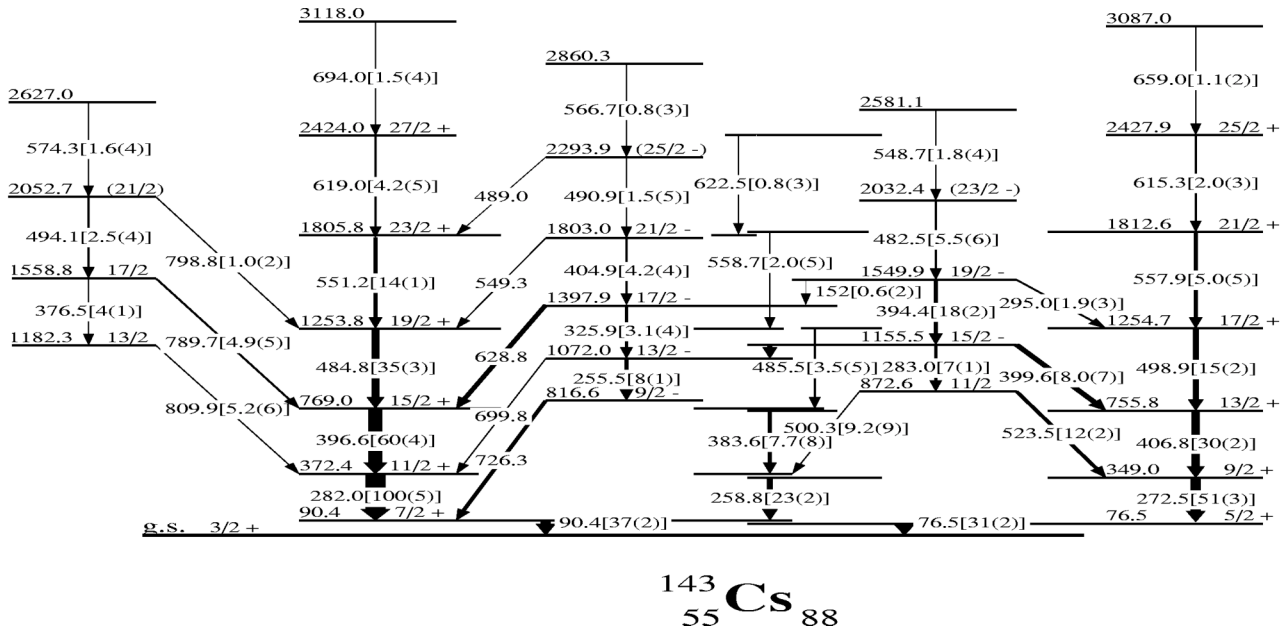

$^{143}_{55}Cs_{88}$

FIG. 3. Partial level scheme of ^{143}Cs as obtained in this work. In square brackets relative γ intensities are given.

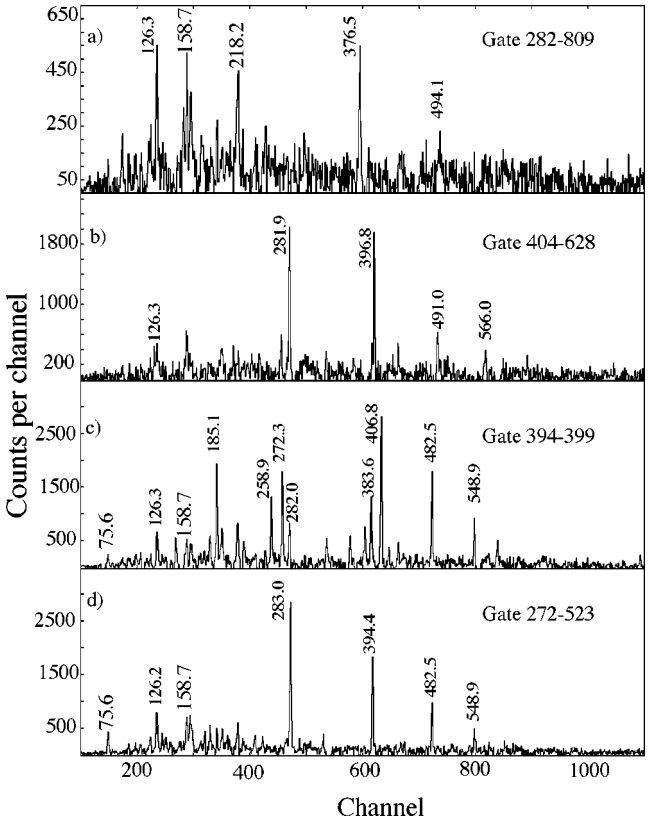

FIG. 4. Coincidence spectra gated on lines corresponding to γ transitions in the ^{143}Cs nucleus, as obtained in this work. Lines at 126 keV, 158 keV, 185 keV, and 218 keV belong to Nb isotopes, the complementary fission fragments.

TABLE II. Angular correlations and linear polarization for transitions in the ^{143}Cs nucleus. "Sum" denotes the summed correlation with more than one yrast-band transition.

$E_{\gamma 1}-E_{\gamma 2}$ (keV–keV)	A_2/A_0	A_4/A_0	$P(E_{\gamma 1})$	Multipolarity of γ_1 transition
76.5–272.5	−0.11(3)	0.02(5)		$\Delta I \leqslant 1$
90.4–282.0	−0.07(3)	−0.01(4)		$\Delta I \leqslant 1$
255.5–325.9	0.10(2)	−0.02(4)		$\Delta I = 2$
258.8–406.8	−0.06(2)	0.06(3)		$\Delta I \leqslant 1$
272.5–406.8	0.07(2)	−0.02(4)		$\Delta I = 2$
283.0–394.4	0.10(4)	0.00(5)		$\Delta I = 2$
325.9–404.9	0.06(3)	−0.04(4)		$\Delta I = 2$
383.6–282.0	−0.06(2)	0.06(4)	−0.09(4)	$M1+E2$
396.6–282.0	0.08(1)	−0.03(2)		$\Delta I = 2$
399.6–sum	−0.11(4)	0.03(6)	+0.08(3)	$E1$
404.9–628.8	−0.10(4)	0.00(4)		$\Delta I \leqslant 1$
484.8–sum	0.09(2)	0.01(1)	+0.12(3)	$E2$
498.9–sum	0.10(3)	0.00(4)	+0.11(4)	$E2$
523.3–272.5	−0.08(1)	0.02(1)	+0.14(8)	$E1$
551.2–sum	0.10(3)	−0.02(2)	+0.07(3)	$E2$
557.9–sum	0.11(3)	0.02(5)		$\Delta I = 2$
615.3–sum	0.10(3)	0.01(5)		$\Delta I = 2$
619.0–sum	0.10(2)	−0.04(3)		$\Delta I = 2$
628.8–sum	−0.08(2)	0.01(3)	+0.26(12)	$E1$
726.3–255.5	−0.12(5)	−0.04(5)		$\Delta I \leqslant 1$
789.7–sum	−0.10(3)	0.01(4)		$\Delta I \leqslant 1$
809.0–282.0	−0.05(2)	−0.02(4)		$\Delta I \leqslant 1$

TABLE III. The $B(E1)/B(E2)$ branching ratios in ^{143}Cs and tentative $B(E1)/B(E2)$ branching ratios in ^{141}Cs, as obtained in this work.

E_{exc} (keV)	$E_\gamma(E1)$ (keV)	$E_\gamma(E2)$ (keV)	$B(E1)/B(E2)$ (10^{-6} fm^{-2})
			^{141}Cs-tentative values
2086.5	603.7	454.7	0.3(1)
2465.2	352.3	524.6	0.21(7)
			^{143}Cs
1072.0	699.8	255.5	0.01(1)
1155.5	399.6	283.0	0.02(1)
1397.9	628.8	325.9	0.01(1)
1549.9	295.0	394.4	0.04(1)
1803.0	549.3	404.9	0.09(2)
2293.9	489.0	490.9	0.07(2)

Q_0 have been taken the same as in the corresponding Xe cores. For ^{140}Xe we have taken $Q_0=1.80(4)$b [12] and for ^{142}Xe $Q_0=2.5(5)$b [13]. Electric dipole moments calculated, using the average $B(E1)/B(E2)$ branching ratios from Table III, are $D_0 \leqslant 0.05(2)e$ fm for ^{141}Cs and $D_0=0.03(1)e$ fm for ^{143}Cs.

The newly found D_0 value in ^{143}Cs and tentative D_0 value in ^{141}Cs are significantly smaller than in their Ba isotones, ^{142}Ba and ^{144}Ba, respectively. This can be seen in Fig. 5, where we show a map of D_0 moments in neutron-rich lanthanides taking D_0 values for Cs isotopes from the present work and for other nuclei from Ref. [13].

The decrease of octupole effects when approaching the $Z=50$ line is expected as a consequence of the existence of a shell gap at $Z=50$. We have shown that this is so, when approaching the $Z=50$ line along the $N=85$ line [14,15]. A similar scenario is suggested for the $N=86$ isotones by the present data on ^{141}Cs and our previous studies of ^{140}Xe [13,16] and ^{138}Te [17]. One concludes therefore, that up to $N=86$ the $Z=50$ gap exists and the lower limit, in the proton number, of the region of octupole deformation in the neutron-rich lanthanides is at $Z=55$. At higher neutron numbers the situation may change, as has been suggested by calculations [18,19], where an increase of the D_0 moment with the increasing neutron number was predicted for Xe isotopes. We have found that in ^{142}Xe the D_0 moment has, indeed, a comparable value to that in ^{144}Ba [13]. On the other hand, the D_0 moment found now in ^{143}Cs, is significantly lower. It remains an open question where is the border line for the octupole deformation and whether the $Z=50$ shell gap still persists at neutron numbers higher than $N=86$.

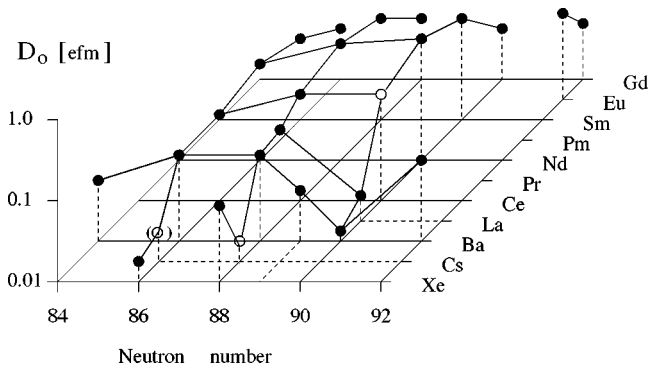

FIG. 5. Values of D_0 moment in the neutron-rich lanthanides. Lines are drawn to guide the eye. Data points for Cs isotopes are found in this work and for other nuclei are taken after Ref. [12].

This work was supported by the Polish Research Council KBN under Grant No. 2P03B02622, by the SERC of the UK under Grant No. GRH71161, and by the U.S. Department of Energy under Contract No. W-31-109-ENG-38.

[1] W. R. Phillips *et al.*, Phys. Rev. Lett. **57**, 3257 (1986).
[2] W. Urban *et al.*, Phys. Lett. B **185**, 331 (1987).
[3] S. Ćwiok and W. Nazarewicz, Nucl. Phys. **A469**, 367 (1989).
[4] T. Rząca-Urban *et al.*, Phys. Lett. B **348**, 336 (1995).
[5] S. H. Faller *et al.*, Phys. Rev. C **38**, 905 (1988).
[6] J. K. Hwang *et al.*, Phys. Rev. C **57**, 2250 (1998).
[7] W. Urban *et al.*, Z. Phys. A **358**, 145 (1997).
[8] W. Urban *et al.*, in *Proceedings of the International Conference on Fission and Neutron-Rich Nuclei, St. Andrews, Scotland 1999*, edited by J. Hamilton and W. R. Phillips (World Scientific, Singapore, 2000), pp. 136–143.
[9] W. Urban *et al.*, Nucl. Instrum. Methods Phys. Res. A **365**, 596 (1995).
[10] M. A. Jones *et al.*, Rev. Sci. Instrum. **69**, 4120 (1998).
[11] W. Urban *et al.*, Nucl. Phys. **A613**, 107 (1997).
[12] S. Raman *et al.*, At. Data Nucl. Data Tables **36**, 1 (1987).
[13] W. Urban *et al.*, Eur. Phys. J. A **16**, 303 (2003).
[14] W. Urban *et al.*, Phys. Rev. C **66**, 044302 (2002).
[15] W. Urban *et al.*, Phys. Rev. C **61**, 041301(R) (2000).
[16] M. Bentaleb *et al.*, Z. Phys. A **354**, 143 (1996).
[17] F. Hoellinger *et al.*, Eur. Phys. J. A **6**, 375 (1999).
[18] W. Nazarewicz and S. L. Tabor, Phys. Rev. C **45**, 2226 (1992).
[19] V. Martin and L. M. Robledo, Phys. Rev. C **49**, 188 (1993).